Communication: SHG-detected circular dichroism imaging using orthogonal phase-locked laser pulses

Jeremy W. Jarrett, Xiaoying Liu, Paul F. Nealey, Richard A. Vaia, Giulio Cerullo, and Kenneth L. Knappenberger Jr.

Citation: The Journal of Chemical Physics **142**, 151101 (2015); doi: 10.1063/1.4918972
View online: http://dx.doi.org/10.1063/1.4918972
View Table of Contents: http://scitation.aip.org/content/aip/journal/jcp/142/15?ver=pdfcov
Published by the AIP Publishing

Communication: SHG-detected circular dichroism imaging using orthogonal phase-locked laser pulses

Jeremy W. Jarrett,[1] Xiaoying Liu,[2] Paul F. Nealey,[2] Richard A. Vaia,[3] Giulio Cerullo,[4] and Kenneth L. Knappenberger, Jr.[1,a)]

[1]*Department of Chemistry and Biochemistry, Florida State University, Tallahassee, Florida 32306-4390, USA*
[2]*The Institute for Molecular Engineering, University of Chicago, Chicago, Illinois 60637, USA*
[3]*Air Force Research Laboratory, 2941 Hobson Way, Wright Patterson Air Force Base, Dayton, Ohio 45433, USA*
[4]*IFN-CNR, Dipartimento di Fisica, Politecnio di Milano, Piazza Leonardo da Vinci 32, 20133 Milano, Italy*

(Received 11 March 2015; accepted 13 April 2015; published online 21 April 2015)

We demonstrate a novel method for second harmonic generation-detected circular dichroism (CD) imaging based on the use of phase-locked, temporally delayed femtosecond laser pulses. The polarization state of the fundamental wave was controllably changed over 2π rad by using a birefringent delay line, which provided attosecond inter-pulse delays for orthogonal phase-locked replicas; the achievable phase stability was 14 as. By introducing either a positive or negative delay of ~667 as, we induced a $\pm\pi/2$ phase shift between the orthogonally polarized pulses, resulting in left circularly polarized or right circularly polarized light. CD imaging performance using the pulse sequence was compared to results obtained for plasmonic nanoantennas using a rotating quarter-wave plate. The pulse sequence is expected to simplify polarization-resolved optical imaging by reducing experimental artifacts and decreasing image acquisition times. This method can be easily extended to other CD spectroscopy measurements. © *2015 AIP Publishing LLC.* [http://dx.doi.org/10.1063/1.4918972]

Nonlinear optical (NLO) imaging is a powerful way to obtain spatially resolved chemical- and material-specific information. The information content obtainable by NLO methods depends upon the image contrast source. Circular dichroism (CD) spectroscopy, which compares the magnitudes of absorption or scattering of right and left circularly polarized light, is a common structure-specific probe. Ultraviolet CD reports on relative amounts of protein secondary structure;[1] vibrational CD is used to determine molecular structure;[2] nonlinear CD has played a pivotal role in the recent emergence of chiro-optical photonic nanomaterials.[3–10] The NLO responses of these materials depend critically upon the precise arrangement of nanoparticles within a network,[3] requiring single-nanostructure measurements. Therefore, CD imaging with high spatial resolution has the much-needed capacity to fill a void in nanophotonics research.

One impediment to CD imaging is the focusing of circularly polarized light to the sample plane of a microscope platform. Conventional microscopes include multi-element high-numerical aperture objectives and dichroic mirrors, which both impart detrimental phase distortion to polarized light that must be compensated for in order to achieve reliable CD imaging.[11] Typically, the polarization state of the incident electromagnetic wave is set using a rotating quarter-wave plate (QWP).[3,7] Imperfections in either the wave plate or its angular rotation can result in erroneous CD data. Other wave-rotating optics such as photoelastic and electro-optic modulators are often used for generating circularly polarized light, but the thickness of these materials and their narrow operational frequency bandwidth (single frequency for photoelastic modulation) limit their use in nonlinear optical imaging and spectroscopy applications that require broad bandwidth coherent light sources. Pulse shapers can be used to control the polarization state of laser pulses, but these methods are technically challenging and expensive.[12]

In this Communication, we demonstrate a novel low-cost and straightforward means of creating left- and right-circularly polarized ultrashort laser pulses for use in nonlinear CD imaging. This method uses a pulse replica generator (PRG) to produce a pair of orthogonal phase-locked laser pulses for which the inter-pulse time delay can be controlled to set the excitation polarization state. We compare CD imaging results for plasmonic assemblies using a traditional CD imaging method that employs a rotating QWP with those acquired using pulse sequences. CD spectroscopy using phase-locked pulses has advantages of rapid data acquisition and artifact-free operation with broad bandwidth laser pulses.

Our experimental CD imaging setup is depicted in Figure 1(a). The excitation source, a mode-locked Ti:sapphire laser (80 MHz, 800 nm center wavelength, 75-nm bandwidth, Coherent Mantis), was circularly polarized using either a QWP or a PRG, as described below. After the polarization state was selected, the fundamental wave was focused onto the sample with a single aspheric lens (numerical aperture, NA = 0.23), and the second harmonic (SH) photons generated from the sample were collected in the transmission direction using a 1.25 NA, 100x oil immersion objective. SH photons were then isolated from the fundamental by a series of optical filters and then focused to the entrance slit of a spectrometer (Andor Technology, Shamrock 303i) coupled to a cooled electron multiplying charge coupled device (Andor Technology, iXon Ultra 897) for imaging.

a)Author to whom correspondence should be addressed. Electronic mail: klk@chem.fsu.edu

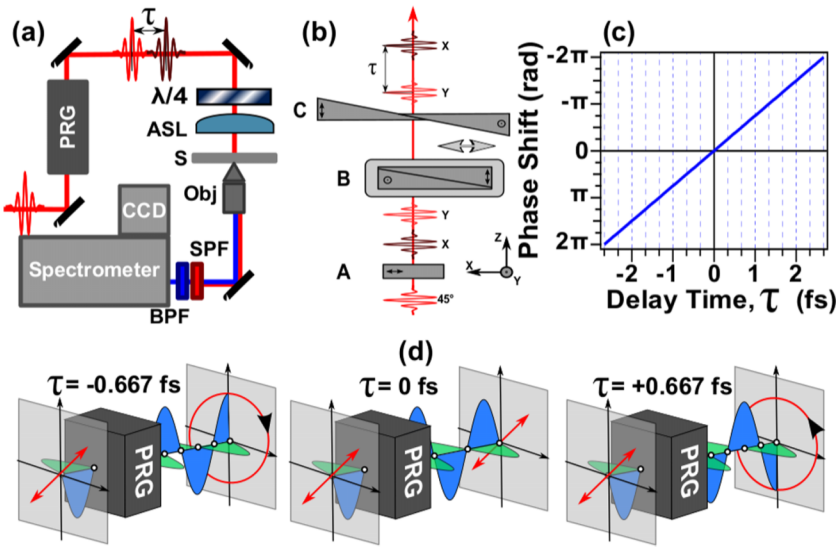

FIG. 1. (a) Optical layout of the NLO microscope. Components included: PRG: pulse replica generator, λ/4: QWP, ASL: aspherical lens, S: sample, Obj.: compound objective lens, SPF: short-pass filter, BPF: band-pass filter. (b) Scheme of the PRG showing the generation of orthogonally polarized replicas with an inter-pulse time delay τ. (c) Calculation of the induced relative phase shift as a function of inter-pulse delay for an 800 nm pulse. (d) Polarization states generated by the indicated inter-pulse delays.

A schematic of the PRG used to generate circularly polarized excitation is shown in Figure 1(b). The setup is derived from the Translating-Wedge-based Identical pulses eNcoding System (TWINS), which is inspired by the Babinet-Soleil compensator, but adapted to ultrabroadband operation.[13] Phase-locked, collinearly propagating pulse replicas were generated by a delay line composed of a sequence of α-BBO birefringent crystals cut and assembled into three blocks (A, B, and C). This sequence of birefringent materials generates a temporal delay between light polarized along the ordinary and extraordinary axes, which can be controlled with extremely high precision (down to 5.7 as) by transverse translation of the block B wedges.

For reference, the input laser source propagated along the z-axis and was linearly polarized 45° with respect to the x-axis. Block A was an 8 mm × 8 mm × 2 mm (xyz) crystal whose optical axis was aligned along the x-axis. Block B consisted of two wedges, with dimensions 16 mm × 8 mm × (0.5-3) mm, assembled such that they overlapped completely (Figure 1(b)). One wedge had the optical axis aligned along the y-axis and the other along the z-axis. This assembly was mounted on a motorized delay stage that traversed the x-axis. Block C was composed of wedges identical to those of block B, however, these wedges only overlapped by the laser beam width.

The laser first passed through Block A, where the incident laser pulse was split into its two orthogonally polarized components, thus forming pulse replicas with a fixed inter-pulse delay time (τ) that depended upon the thickness of crystal A (d_A). Next, these replicas passed through block B, affecting only the y-polarized replica. Translating block B along the x-axis moved the y-polarized replica in time by changing the thickness of the crystal whose optical axis was oriented along the y-axis (d_B). Block C served to compensate for the angular dispersion introduced by the wedges of block B. The inter-pulse delay time is a function of the amount of birefringent material inserted and the refractive indexes of the ordinary and extraordinary axes of the material [$(\tau = (d_A - d_B)\delta_{eo}$, where $\delta_{eo} = (1/v_{ge}) - (1/v_{go})$ and $v_{ge}(v_{go})$ is the group velocity along the extraordinary(ordinary) axis]. In our setup, the maximum temporal separation between pulses occurred when block B was completely inserted, corresponding to an inter-pulse separation of 466.67 fs. The minimum time step depended upon the precision of the delay stage on which block B moved. The precision of our stage was 0.1 μm, corresponding to a minimum time step of 5.7 as with our crystal parameters. The induced temporal delays were calibrated using He-Ne interferometric tracking. Since the overall material thickness of the PRG does not change upon block B translation, the pulse duration of the replicas does not change.

In order to generate a circularly polarized fundamental source, the two orthogonal pulse replicas must have an inter-pulse delay of one-quarter wave (π/2-phase shift). The PRG can be used to generate these conditions (Figure 1(d)). Here, we demonstrate that introducing inter-pulse temporal delays of −0.667, 0, and +0.667 fs between phase-locked orthogonal pulse replicas generates left circular, linear, and right circular polarization states of light, respectively. Figure 1(c) shows the anticipated phase shift as a function of pulse delay time. The attosecond delays achievable using the PRG allow a multitude of phase shifts to be induced; we generated output light that was horizontally, vertically, elliptically, or circularly polarized, depending on the position of block B.

A key feature of the PRG device is its ability to generate broad bandwidth replicas that are phase-locked with high stability, while preserving the short temporal duration of the parent femtosecond pulse.[13] The phase stability of the replicas was characterized by spectral interferometry. Pulse durations were typically sub-30 fs with pre-compensation for dispersion. A sequence of high-contrast fringe patterns recorded over a 2 h period with fixed wedges is presented in Figure 2(a). The fringes are obtained by projecting the two replicas on the same polarization direction by a linear polarizer, for a delay τ = 430 fs. Figure 2(b) shows the extracted relative phase measured over this time course. The trace had rms fluctuations of ~33 mrad, corresponding to delay fluctuations of ~14 as or ~1/190th of an optical cycle at 800 nm. The observed phase jitter translated to a 2% fluctuation in the π/2 phase shift needed to generate circularly polarized light. Overall, this measurement provided direct evidence for the long-lived high phase stability of the PRG. Combining the phase stability with

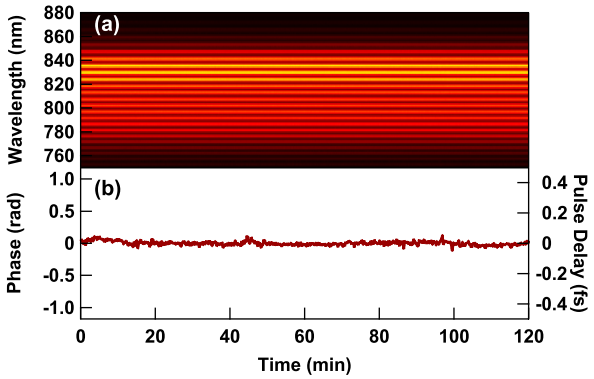

FIG. 2. (a) Sequence of fringe patterns acquired while keeping the wedge position fixed for 2 h. (b) Phase fluctuations extracted from (a). The phase jitter was less than 1/190th of an optical cycle.

the delay step precision of 5.7 as, we could reliably produce the polarization states necessary to perform CD imaging, which required inter-pulse time delays of 667 as.

In Figure 3, we demonstrate our ability to use the PRG to change the input source polarization state. Figure 3(a) portrays the laser power measured after the PRG as the inter-pulse delay time was varied and the output was analyzed using a linear polarizer, graphically depicting accessible polarization states for delays spanning −1.33 fs to +1.33 fs sampled at 30-as intervals. This delay range corresponded to a π phase shift between the two pulses in both time directions (1/2-wave rotation). Figure 3(b) depicts slices of the data from Figure 3(a) at time delays of 0, +0.40, and +0.67 fs, which correspond to linear, elliptical, and circular polarization states. The black trace, taken at 0 time delay, showed a dipolar pattern and corresponded to linearly polarized light. The light blue trace represents data obtained using a +0.40 fs inter-pulse time delay; it has more intensity in the orthogonal direction than the black trace, reflective of an elliptical polarization state. The red trace shows no change in measured laser power, regardless of the analyzer rotation angle, and it thus depicts circular polarization. We analyzed the degree of circular polarization over the entire spectral bandwidth of the pulse and found it to be uniformly polarized. In Figure 3(c), we show data collected at −1.33 (black), −1.06 (blue), and −0.67 (green) fs time delays. Generation of a −1.33 fs time delay between two orthogonal phase-stable 800-nm pulse pairs is equivalent to inducing a 1/2-wave (π-phase shift) rotation with respect to the pulse pair at zero time delay. The black trace in Figure 3(c) depicts a linear polarization state, oriented orthogonal

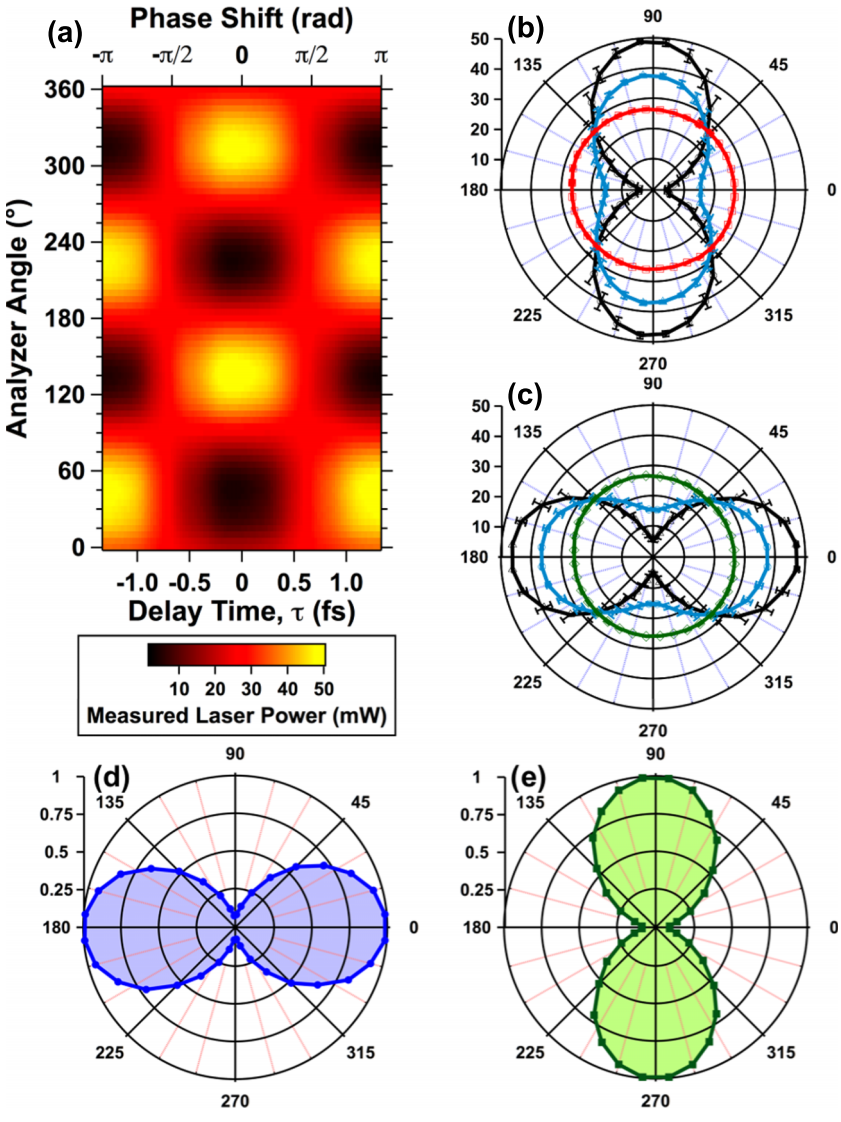

FIG. 3. (a) Colormap of measured output power from PRG as a function of linear polarizer analyzer angle and inter-pulse delay time. (b) Vertical slices from (a) along delay times of 0 fs (black), +0.40 fs (blue), and +0.67 fs (red). (c) Slices along delay times of −1.33 fs (black), −1.06 fs (blue), and −0.67 fs (green). (d) RCP and (e) LCP light generated at +0.67 and −0.67 fs analyzed with a QWP/LP set. Orthogonal orientation confirmed that LCP and RCP light is generated.

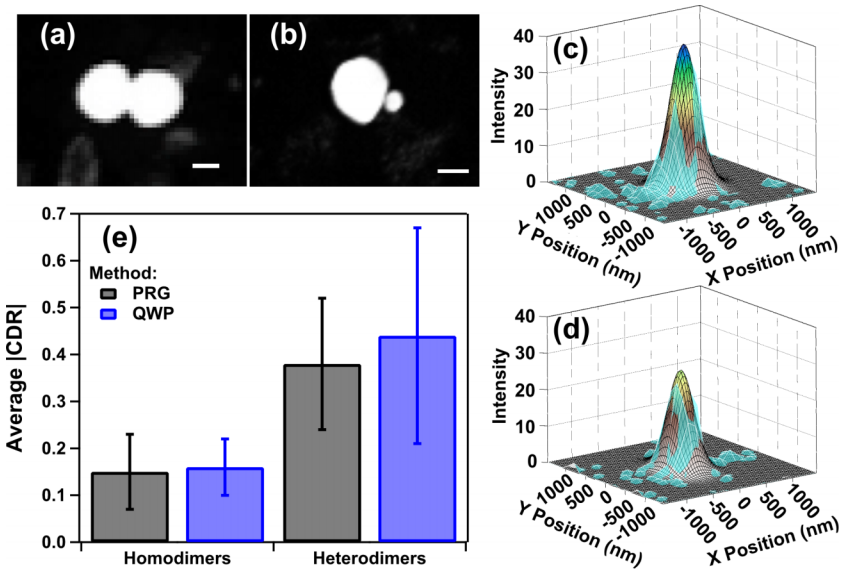

FIG. 4. ((a) and (b)) Representative SEM images of the two different nanoparticle systems studied: (a) homodimer and (b) heterodimer nanoclusters. The scale bars represent 100 nm. ((c) and (d)) SHG data generated from LCP (c) and RCP (d) excitation of gold nanosphere heterodimers. (e) Comparison of average SHG-CDR values obtained for two different nanoparticle systems generated from two different methods, QWP and PRG.

to the dipolar pattern obtained using zero inter-pulse time delay (Figure 3(b); black trace). These experimental results confirmed predictions based on the inter-pulse time delay. The blue trace was generated using an inter-pulse time delay of −1.06 fs. Under this condition, the fundamental wave was elliptically polarized with the major axis of the ellipse along the x-axis (i.e., orthogonal to the blue trace in Figure 3(b)). The green trace portrays the measured laser power generated at −0.67 fs inter-pulse delay, which corresponded to a $\pi/2$ phase shift, generating a circularly polarized fundamental wave. Taken together, these data demonstrated that controlling the inter-pulse delay between orthogonal phase-locked laser pulses allowed the PRG to function as an efficient variable wave plate.

We analyzed the circularly polarized PRG-produced light with a quarter-wave plate/linear polarizer (QWP/LP) combination to ensure that both left- and right-handed polarization states were generated. The QWP transformed the circularly polarized light back into linearly polarized light, and the polarization angle was measured with a linear polarizer. We first translated the block B motor to −0.67 fs to produce circularly polarized light. Then, we analyzed this light with the QWP/LP combination and observed a dipolar pattern with the major axis aligned along the x-axis at 0° (Figure 3(d)). This confirmed circular polarization of the light, and we denoted this light as left circularly polarized (LCP). Then, keeping the quarter-wave plate fixed, we translated the motor to +0.67 fs and measured the laser power as the linear polarizer was rotated. We again observed a dipolar intensity pattern, but with the major axis along the y-axis at 90°. These results indicated a different handedness to the polarized light (i.e., polarization state), and we denoted this configuration as right circularly polarized (RCP). Taken together, these data demonstrated our ability to produce light of many polarization states, specifically the LCP and RCP necessary for CD imaging.

To demonstrate the effectiveness of the pulse replicas for CD imaging, the LCP and RCP light generated from the PRG was used to perform second harmonic generation (SHG)-detected CD imaging on plasmonic gold nanoparticle (GNP) dimers. GNP heterodimers were chosen for this demonstration because they exhibit non-zero CD owing to a combination of interfacial chirality and inter-particle dipolar and multi-polar interference.[3,14] SEM images of the heterodimer and homodimer nanoparticle systems are displayed in Figures 4(a) and 4(b), respectively. The homodimer system contained two gold metal nanoparticles (MNPs) with 150 nm diameter separated by a 1–10 nm gap, and the heterodimer system consisted of two gold MNPs with 150 and 50 nm diameters separated by a 1–10 nm gap. Sample preparation and characterization details have been reported previously.[15]

Differential CD is reported as the SHG circular difference ratio (SHG-CDR) given by $|SHG - CDR| = |2(I_{2\omega}^{LCP} - I_{2\omega}^{RCP})/(I_{2\omega}^{LCP} + I_{2\omega}^{RCP})|$, where $I_{2\omega}$ is the number of SHG photons imaged with LCP and RCP excitation.[16] Figures 4(c) and 4(d) show the SHG-CDR from a gold heterodimer nanoparticle assembly. A large, unambiguous difference in intensity was observed upon excitation with LCP versus RCP. The corresponding SHG-CDR for this particle was calculated as 0.35. The total acquisition time for CD images included both the required exposure time and the time needed to switch between LCP and RCP excitation. Computer-controlled linear translation of the PRG allowed for rapid changing of the polarization state, thus reducing the image acquisition time by a factor of 8 when compared to motorized wave plate rotation. Furthermore, rapid transformation of the fundamental polarization between LCP, RCP, and linear polarization states and construction of image statistics for individual particles was obtained via computer programming. As a result, the reproducibility of the measurements could be analyzed by sampling polarization states in an arbitrary sequence. The rapid acquisition time is also important for imaging heterogeneous nanoparticles, for which microscope stability is a limiting factor.

To test PRG performance, we measured the average SHG-CDR of two different GNP systems and compared the results obtained using both the PRG and a QWP for generation of left and right circularly polarized excitation. Data were compared for 5 different heterodimer samples and 12 different homodimer samples using QWP and PRG for excitation (Figure 4(e)). For the heterodimers, the QWP

method produced an average SHG-CDR value of 0.44 ± 0.23, and the PRG method produced an average value of 0.38 ± 0.16. For the homodimers, the average values were 0.16 ± 0.06 (QWP) and 0.15 ± 0.08 (PRG). The non-zero SHG-CDR values obtained for homodimers were attributed to the inherent heterogeneity of the nanosphere building blocks, which caused an asymmetric inter-particle interface.[3] The comparatively large SHG-CDR values for the heterodimers were attributed to interference between quadrupolar and dipolar modes of the 150-nm and 50-nm nanospheres, respectively.[15] The results from these two independent methods were within error of each other, showing the PRG to be a viable means to produce the excitation source necessary for CD imaging. Moreover, the short acquisition times and ease of transforming the laser polarization state allow for rapid diffraction-limited (≈160-nm resolution) CD imaging and single-particle spectroscopy. Statistical localization analysis of the SHG data allows pinpointing the position of the signal point source with nanometer accuracy.

We performed SHG-CDR experiments operating in transmission geometry to avoid detrimental phase shifts induced by the dichroic mirrors and multi-element compound objectives used in epi-collection microscopes. We found that light reflection by a dichroic mirror changed the polarization state from circular to elliptical. Using the PRG, we pre-compensated for this shift by changing the time delay between pulses to achieve circular polarization states after the dichroic mirror.

In conclusion, a novel and simple means to produce circularly polarized broad-bandwidth excitation for nonlinear optical CD imaging applications was presented. We demonstrated a phase-locked pulse pair generator based on TWINS technology that could change the polarization state by introducing inter-pulse time delays between orthogonally polarized pulse replicas, providing user control over the phase relationship of the pulse replicas. We compared the circular dichroism ratios obtained for chiro-optically active plasmonic nanoparticle assemblies using the PRG to data resulting from use of a traditional wave plate and concluded that using phase-locked, orthogonal laser pulses with controlled inter-pulse time delays set by the PRG was a reliable approach for generating excitation sources for CD imaging. In fact, controlling the inter-pulse time delay of the pulse pairs proved as effective as a functional wave plate for generating many different excitation polarization states. Significant advantages of the pulse replica method over wave plates include programmed control over the inter-pulse delays, rapid and high through-put image acquisition, and artifact-free polarization manipulation over 2π rad. We expect that the use of phase-locked pulse replicas for polarization-resolved optical imaging will find widespread use in many nonlinear optical imaging and spectroscopy applications.

This work was supported by an award from the National Science Foundation (NSF), Grant No. CHE-1150249, to K.L.K. and the European Research Council Advanced Grant STRATUS (ERC-2011-AdG No. 29119) to G.C.

[1]J. P. Hennessey and W. C. Johnson, Biochemistry **20**, 1085 (1981).
[2]T. B. Freedman, X. L. Cao, R. K. Dukor, and L. A. Nafie, Chirality **15**, 743 (2003).
[3]M. Chandra, A. M. Dowgiallo, and K. L. Knappenberger, Jr., J. Am. Chem. Soc. **134**, 4477 (2012).
[4]M. Chandra and K. L. Knappenberger, Jr., Phys. Chem. Chem. Phys. **15**, 4177 (2013).
[5]J. W. Jarrett, P. J. Herbert, S. Dhuey, A. M. Schwartzberg, and K. L. Knappenberger, Jr., J. Phys. Chem. A **118**, 8393 (2014).
[6]M. Kauranen, T. Verbiest, J. J. Maki, and A. Persoons, J. Chem. Phys. **101**, 8193 (1994).
[7]M. Kauranen, T. Verbiest, and A. Persoons, J. Mod. Opt. **45**, 403 (1998).
[8]J. J. Maki, M. Kauranen, and A. Persoons, Phys. Rev. B **51**, 1425 (1995).
[9]V. K. Valev, J. J. Baumberg, C. Sibilia, and T. Verbiest, Adv. Mater. **25**, 2517 (2013).
[10]V. K. Valev, A. V. Silhanek, N. Verellen, W. Gillijns, P. Van Dorpe, O. A. Aktsipetrov, G. A. E. Vandenbosch, V. V. Moshchalkov, and T. Verbiest, Phys. Rev. Lett. **104**, 127401 (2010).
[11]Y. Q. Tang, T. A. Cook, and A. E. Cohen, J. Phys. Chem. A **113**, 6213 (2009).
[12]T. Brixner and G. Gerber, Opt. Lett. **26**, 557 (2001).
[13]D. Brida, C. Manzoni, and G. Cerullo, Opt. Lett. **37**, 3027 (2012).
[14]X. R. Tian, Y. R. Fang, and B. L. Zhang, ACS Photonics **1**, 1156 (2014).
[15]S. Biswas, X. Y. Liu, J. W. Jarrett, D. Brown, V. Pustovit, A. Urbas, K. L. Knappenberger, Jr., P. F. Nealey, and R. Vaia, Nano Lett. **15**, 1836 (2015).
[16]J. W. Jarrett, M. Chandra, and K. L. Knappenberger, Jr., J. Chem. Phys. **138**, 214202 (2013).